PRAMANA
— journal of
physics

Vol. 65, No. 4
October 2005
pp. 593–599

Negative differential resistance in a one-dimensional molecular wire with odd number of atoms

S LAKSHMI and SWAPAN K PATI
Theoretical Sciences Unit, Jawaharlal Nehru Centre for Advanced Scientific Research, Jakkur P.O., Bangalore 560 064, India
E-mail: pati@jncasr.ac.in

Abstract. We have investigated the effects of electron–phonon coupling on the current–voltage characteristics of a one-dimensional molecular wire with odd number of atoms. The wire has been modelled using the Su–Schreiffer–Heeger (SSH) Hamiltonian and the current–voltage characteristics have been obtained using the Landauer's formalism. In the presence of strong electron–lattice coupling, we find that there are regions of negative differential resistance (NDR) at some critical bias, due to the degeneracy in the energies of the frontier molecular orbitals. The presence of the applied bias and the electron–lattice coupling results in the delocalization of these low-lying molecular states leading to the NDR behaviour.

Keywords. Molecular wire; electron–phonon; Su–Schreiffer–Heeger Hamiltonian; Landauer; Newns–Anderson.

PACS Nos 72.23.-b; 72.23.Hk; 73.63.-b; 85.65.+h

1. Introduction

A molecule attached between two macroscopic electrodes has evinced a lot of interest in the past few years [1]. A large number of experimental and theoretical work have been performed to understand transport in such systems. Single molecules attached between electrodes have already been demonstrated to show conducting, rectifying and switching behaviour [2–7]. A variety of theoretical methods ranging from semi-empirical to density functional theory (DFT) based methods [8–14] have been explored to describe transport properties in such nanoscale systems. The problem, although interesting both from a fundamental point of view and in terms of device applications in the electronics industry, is quite complex. Most descriptions until now have been developed within some simple approach neglecting entirely the inelastic scattering in the molecule [1].

Inelastic processes include electron–electron, electron–phonon and impurity mediated scatterings. In this paper, we neglect the scattering due to electron–electron interactions and consider the transport properties in the presence of underlying

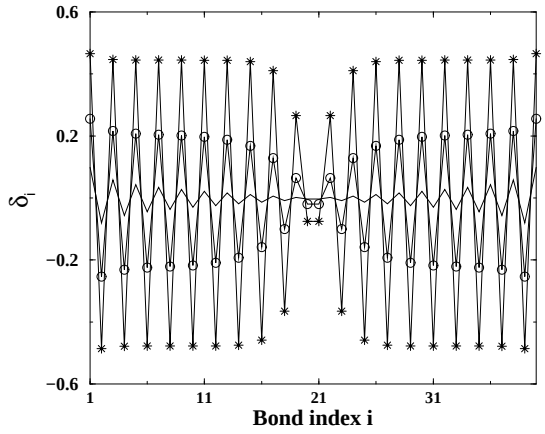

Figure 1. Variation of the bond-alternation parameter (δ_i) with bond index, i, for different values of λ: $\lambda = 0.5$ (solid line), $\lambda = 1$ (circles) and $\lambda = 1.5$ (stars).

lattice distortions, of a one-dimensional molecular wire with odd number of atomic sites. The wire is described by the SSH Hamiltonian [15], where the electrons are treated within a tight-binding description and the phonons are treated adiabatically. The wire–electrode coupling is calculated within the Newns–Anderson chemisorption [16] model. Since the inelastic interactions included do not result in a loss of coherence of the tunneling electrons, we employ the Landauer's scattering approach to calculate the current–voltage characteristics [17].

2. Computational strategy

The computational method we have employed, has been described in detail elsewhere [10]. Here we give only the essential details. The one-dimensional molecular wire has been modelled as a half-filled polyene chain with odd number of atomic sites. It is described by the Su–Schreiffer–Heeger (SSH) Hamiltonian which captures the effect of electron–phonon coupling in a simplistic way. The Hamiltonian is rewritten from its original form as

$$H = \sum_i -(1+\delta_i)(a_i^\dagger a_{i+1} + hc) + \frac{1}{\pi\lambda}\sum_i \delta_i^2, \tag{1}$$

where the first term describes the hopping of π electrons along the polyene chain without spin flip. δ is the bond-alternation parameter which renormalizes the electron hopping strength by the displacement of the underlying atoms and is dependent on the strength of the electron–phonon coupling. λ is a dimensionless coupling constant defined as $\lambda = 2\alpha^2/\pi K t^2$ where t is the π electron hopping integral, K and α are the elastic spring constants associated with the nuclear motion and the electron–phonon interactions respectively. An expression for δ is obtained by minimizing the

above Hamiltonian with the constraint that the energy changes associated with the net displacement about the mean positions should be zero so that the total length of the wire remains a constant:

$$\delta_i = \frac{\pi\lambda}{2}[\langle a_i^\dagger a_{i+1} + hc\rangle - \frac{1}{N}\sum_i \langle a_i^\dagger a_{i+1} + hc\rangle], \tag{2}$$

where N is the total number of bonds. In our calculations, we start with an initial guess for the δs and solve for the Hamiltonian of the wire in the absence of any external bias. We then calculate bond orders which essentially gives δ, thus solving self-consistently until all the bond orders converge. From the eigenenergies of this relaxed system the Fermi energy (E_{F}) of the electrodes is calculated assuming that it falls mid-way between the equilibrium HOMO and LUMO energies for the molecule alone. Assuming this pattern of δs as the equilibrium configuration, we proceed to study the effect of external bias on the wire. The applied bias is assumed to be a ramp function. The effect of the electrodes is incorporated using the Newns–Anderson model for chemisorption between the atoms of the wire and the electrode. The molecular Hamiltonian gets modified by the self-energies due to the electrodes as $\bar{H} = H + \Sigma_1 + \Sigma_2$ where Σ_1 and Σ_2 are the self-energies corresponding to the two electrodes. Once the effective Hamiltonian for the electrode–molecule–electrode is obtained, the current through the wire is calculated using the Landauer's formula

$$I(V) = \frac{2e}{h}\int_{E_{\mathrm{F}}-eV}^{E_{\mathrm{F}}} \mathrm{d}E\,[\mathrm{Tr}(\Gamma_1 G \Gamma_2 G^\dagger)], \tag{3}$$

where $\Gamma_{1,2}$ are the anti-hermitian parts of the self-energy matrices, $\Gamma_{1,2} = i(\Sigma_{1,2} - \Sigma_{1,2}^\dagger)$ which describe the broadening of the energy levels due to coupling to the electrodes. The Green's function G is obtained as the inverse of the modified Hamiltonian, $G(E) = 1/(EI - H - \Sigma_1 - \Sigma_2)$ and hence the current is calculated.

3. Results and discussions

Before we discuss the non-equilibrium results, we give a quantitative idea of the distortions caused in the system due to the presence of electron–phonon coupling. Figure 1 shows the bond length distortions, δs, against the bond positions for a range of dimensionless couplings λ, for a 41-site wire. A noticeable feature is the kink appearing at the middle of the chain affirming the fact that the ground state of an odd-site system is a solitonic state. As the coupling strength is increased, the chain is more and more distorted, however, in this process, the system gains some additional energy. This is the Peierls dimerization mechanism [18] which causes the system to open up a gap near the Fermi energy thereby making the system less conducting. This non-conducting gap increases as the coupling strength is increased. For $\lambda = 1$, we find that the HOMO–LUMO gap is about 0.9 eV. For all our calculations, we have used this value of the electron–phonon coupling unless otherwise stated.

Figure 2 shows the equilibrium density of states and transmission for this half-filled wire, with $\lambda = 1$ and $\lambda = 0$ (non-interacting case). The peaks in the DOS

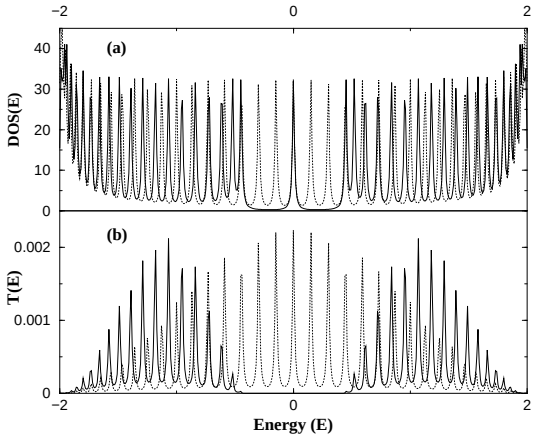

Figure 2. (**a**) Density of states DOS(E) and (**b**) transmission $T(E)$ in equilibrium condition (zero bias), for the non-interacting case ($\lambda = 0$, dashed lines) and with electron–phonon coupling ($\lambda = 1$, solid lines).

represent the positions of the energy levels and the presence of a zero energy peak in the presence of strong electron–phonon coupling, indicating the appearance of the solitonic level. This state has zero energy because the kink essentially splits the chain into two halves removing all interactions amongst them. Figure 2b shows that in the presence of electron–phonon coupling, the Peierls' gap splits the transmission peaks clearly into two bands about E_{F}. And on either side of the gap, the transmission shows a band-like picture with maximum transmission at the middle of each of the bands. The solitonic state also shows negligible transmission along with the other states around E_{F} indicating that the levels which are most important for transport are localized even at zero bias, in the presence of electron–lattice coupling.

Now we look at the effect of external bias on the non-equilibrium current–voltage characteristics of the system. As mentioned earlier, the potential profile across the molecule–electrode system is considered as a ramp function. Figure 3 compares the I–V of a non-interacting chain ($\lambda = 0$) with that in the presence of strong electron–lattice coupling ($\lambda = 1$). In the former case, the current increases by jumps, well-known as the eigenvalue staircase picture [19], occurring whenever the Fermi energy of the electrodes crosses the molecular energy levels. It can be seen that the first jump in current occurs as soon as a small bias is switched on. This is because for an odd-site wire, the Fermi energy of the electrodes coincides with the solitonic level which is not localized in the absence of the electron–phonon coupling. However when the electron–phonon interaction is switched on, the current shows sharp negative differential resistance (NDR) at some large bias, in the off-resonant condition. Two such peaks can be seen in the figure, at voltages of around 1.6 V and 2.0 V for this 41-atomic chain. The second peak is noticeably sharper and interestingly, the value of current at that bias is equal to the non-interacting current.

To understand the nature of this NDR and its origin, we compute the one-electron Greens function, which determines the magnitude and nature of the current–voltage

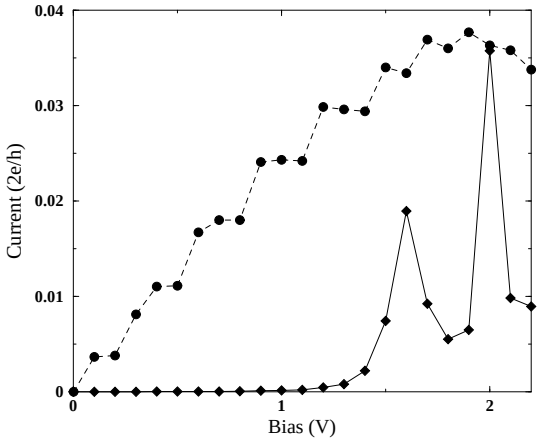

Figure 3. The current–voltage characteristics for a 41-atomic sites wire for the non-interacting case ($\lambda = 0$, circles) and with electron–phonon coupling ($\lambda = 1$, diamonds).

characteristics. The Greens function element, expanded in the basis of molecular orbitals can be written as $G_{1N} = \sum_k \frac{C_{1k}C_{Nk}}{E-E_k+i\eta}$, where the C_{mk}'s are the kth molecular eigenvector coefficients corresponding to the mth atomic site of the wire, and E_k is the energy of the kth molecular level. Figure 4a shows the energies of a few selected molecular orbitals close to the zero of energy as a function of the applied bias. It can be seen that in general, all the levels decrease linearly with bias at small bias strength. But at a bias of around 1.6 V, the HOMO and LUMO levels come very close to the SOMO (singly occupied molecular level or solitonic level) after which they move farther apart. Then at a bias of around 2.0 V, the HOMO and HOMO-1 (and due to electron–hole symmetry, the LUMO and LUMO+1) levels come close to each other. In figure 4b, we have plotted the numerators of the Greens function, which are the products of the coefficients $C_{1k}C_{Nk}$, for the corresponding four k states shown in figure 4a. They determine the nature of the current characteristics in the off-resonant condition, regions in the vicinity of the poles of the Greens function. As can be seen, the numerator values increase at the critical bias regions where the corresponding energy levels show quasi-degeneracy (see figure 4a). We have also computed the average inverse participation ratio ($\mathrm{IPR_{av}}$), defined as, $\mathrm{IPR_{av}} = \frac{1}{D(E)}\frac{1}{N}\sum_k P_k^{-1}\delta(E-E_k)$ where P_k^{-1} is the inverse participation ratio (IPR) and $D(E)$ is the density of states. IPR is defined as: $P_k^{-1} = \frac{1}{N}\sum_j |\psi(j,k)|^4$ where the indices k and j correspond to the molecular orbitals and the atomic sites respectively. IPR defines the extent of localization for a given eigenstate. In figure 4c, we have plotted $\mathrm{IPR_{av}}$ as a function of the applied bias for the corresponding states discussed in figures 4a and 4b. It is very clear that at the bias at which NDR was observed, there is a dip in $\mathrm{IPR_{av}}$ indicating delocalized nature of the states.

Let us discuss these features in some simple form. In the presence of electron–phonon coupling, the system with odd number of atoms becomes dimerized with a kink in the middle. This state corresponds to the SOMO. The HOMO and LUMO

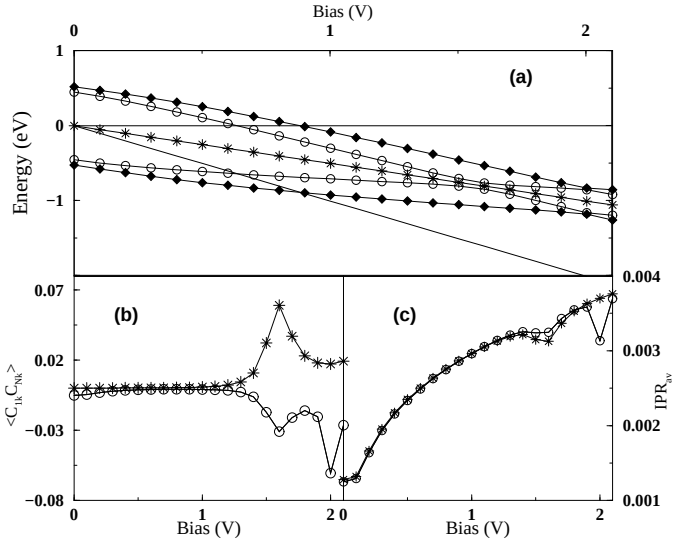

Figure 4. (**a**) The variation of the Fermi energies of the electrodes (thick solid lines) and of the HOMO-1 (diamonds), HOMO (circles), SOMO (stars), LUMO (circles) and LUMO+1 (diamonds) levels, with the external bias (for $\lambda = 1$). Same symbol for different states if they have the same symmetry. The Fermi energy of one electrode is kept at a constant value and that of the other electrode is varied with the bias. (**b**) The numerator of the Greens function matrix element for the corresponding energy levels shown in (a). The index k specifies the corresponding molecular orbital and 1 and N are the first and the last sites of the wire. (**c**) The average inverse participation ratio for the SOMO, HOMO and LUMO levels.

are the mirror reflections of each other (in terms of dimerizations) and have the same parity. One part of the SOMO resembles the HOMO and the other part resembles the LUMO. When bias is applied, both the HOMO and LUMO approach each other and the SOMO. At some critical bias (1.6 V), all these three states are so close in energy that a mixing of the SOMO with HOMO and SOMO with LUMO occurs (HOMO and LUMO do not mix as they are of the same parity) leading to a delocalization and hence a rise in current. Beyond this critical bias, since the HOMO and LUMO states have acquired some characteristics of the SOMO, they start moving away. This results in localization again and a fall in the magnitude of current. Interestingly, at around 2.0 V, when the HOMO and HOMO-1 (LUMO and LUMO+1) levels come close, since they are of opposite parity, they can mix and the system becomes delocalized with all its bond lengths equal. This is precisely why the current at this bias is equal to the non-interacting wire current. The main factor affecting the critical bias is the initial gap of the system which depends directly on the size of the system and inversely on the strength of the electron–phonon coupling.

In conclusion, we have provided an alternate explanation for NDR that has been observed in many organic systems. Some of the explanations proposed in literature vary from charging effects [20,21] and conformational changes [10,22,23] to bias

induced changes in molecule–electrode coupling [24]. Our explanation for the origin of NDR is quite general and independent of molecule–electrode coupling strength and location of the Fermi energy. More work is required to find any common link among all the theories for a clear understanding of NDR in nanoscale systems.

Acknowledgements

SKP acknowledges the DST, Government of India, for financial support.

References

[1] F Zahid, M Paulsson and S Datta, *Electrical conduction through molecules*, *Advanced semiconductors and organic nano-techniques* edited by H Morkoc (Academic Press, 2003)
[2] M A Reed, C Zhou, C J Muller, T P Burgin and J M Tour, *Science* **278**, 252 (1997)
[3] J Chen, W Wang, M A Reed, A M Rawlett, D W Price and J M Tour, *Appl. Phys. Lett.* **77**, 1224 (2000)
[4] J M Tour, *Acc. Chem. Res.* **33**, 791 (2000)
[5] J Chen, M A Reed, A M Rawlett and J M Tour, *Science* **268**, 1550 (2001)
[6] S J Tans, M H Devoret, H Dai, A Thess, R E Smalley, L J Geerligs and C Dekker, *Nature (London)* **386**, 474 (1997)
[7] J G Kushmerick, D B Holt, S K Pollack, M A Ratner, J C Yang, T L Schull, J Naciri, M H Moore and R Shashidhar, *J. Am. Chem. Soc.* **124**, 10654 (2002)
[8] P S Damle, A W Ghosh and S Datta, *Phys. Rev.* **B64**, 201403 (2001)
[9] Eldon G Emberly and G Kirczenow, *Phys. Rev.* **B64**, 235412 (2001)
[10] S Lakshmi and Swapan K Pati, *J. Chem. Phys.* **121**, 11998 (2004)
[11] T Tada, D Nozaki, M Kondo, S Hamayama and K Yoshizawa, *J. Am. Chem. Soc.* **126**, 14182 (2004)
[12] Y Xue and M A Ratner, *Phys. Rev.* **B70**, 081404 (2004)
[13] Y C Chen, M Zwolak and M Di Ventra, *Nano Lett.* **4**, 1709 (2004)
[14] F Zahid, A W Ghosh, M Paulsson, E Polizzi and S Datta, *Phys. Rev.* **B70**, 245317 (2004)
[15] W P Su, J R Schreiffer and A J Heeger, *Phys. Rev. Lett.* **42**, 171 (1979), *Phys. Rev.* **B22**, 2099 (1980)
[16] P W Anderson, *Phys. Rev.* **124**, 41 (1961)
D M Newns, *Phys. Rev.* **178**, 1123 (1969)
[17] M Buttiker and R Landauer, *Phys. Rev. Lett.* **49**, 1739 (1982); *Phys. Scr.* **32**, 429 (1985)
[18] R E Peierls, *Quantum theory of solids* (Clarendon Press, Oxford, 1955)
[19] V Mujica, M Kemp, A E Roitberg and M A Ratner, *J. Chem. Phys.* **104**, 7296 (1996)
[20] J M Seminario, A G Zacarias and J M Tour, *J. Am. Chem. Soc.* **122**, 3015 (2000)
[21] J M Seminario, A G Zacarias and P A Derosa *J. Chem. Phys.* **116**, 1671 (2002)
[22] J Cornil, Y Karzazi and J L Bredas, *J. Am. Chem. Soc.* **124**, 3516 (2002)
[23] R Pati and S P Karna, *Phys. Rev.* **B69**, 155419 (2004)
[24] X Shi, X Zheng, Z Dai, Y Wang and Z Zeng, *J. Phys. Chem.* **B109**, 3334 (2005)